Time-dependent Optimal Heater Control in Thermoforming Preheating Using Dual Optimization Steps

Zhen-Zhe Li[1], Kwang-Su Heo[1] and Seoung-Yun Seol[1,#]

1 Department of Mechanical Engineering, Chonnam National University, 300, Yongbong-dong, Buk-gu, Gwangju, South Korea, 500-757
Corresponding Author / E-mail: syseol@chonnam.ac.kr, TEL: +82-62-530-1678, FAX: +82-62-530-1689

KEYWORDS: Thermoforming, Optimum design, Response surface Method, Heat transfer

Thermoforming is one of the most versatile and economical processes available for shaping polymer products, but obtaining a uniform thickness of the final product using this method is difficult. Heater power adjustment is very important because the thickness distribution depends strongly on the distribution of the sheet temperature. In this paper, the steady-state optimum distribution of heater power is first ascertained by a numerical optimization to obtain a uniform sheet temperature. The time-dependent optimal heater input is then determined to decrease the temperature difference through the direction of the thickness using the response surface method and the D-optimal method. The optimal results show that the time-dependent optimum heater power distribution gives an acceptable uniform sheet temperature in the forming temperature range by the end of the heating process.

Manuscript received: January 7, 2008 / Accepted: May 15, 2008

NOMENCLATURE

A_s = area of the ABS sheet
C_P = specific heat of the ABS sheet
c = coefficient of the response surface
$F_{k\,j}$ = view factor from the kth element to the jth element
g = acceleration of gravity
h = convective heat transfer coefficient
J = radiosity
k = thermal conductivity of the ABS sheet
L = characteristic length
m = mass
N = total number of heater and sheet elements
n_h = number of heaters
P = circumference
q_{elec} = power to the heater
q_h = heat flow rate of the heater
q'_{conv} = convective heat flux
q'_{in} = heat flux input
q'_{rad} = radiation heat flux
q'_{req} = required heat flux
Ra_L = Rayleigh number
T_i = initial temperature
T_f = final temperature
T_∞ = environmental temperature
t_h = heating time
υ = dynamic viscosity of air
x = design variable
z = position coordinate
β = volume expansion coefficient of air
ρ = density of the ABS sheet
σ = Stefan–Boltzmann constant
ε = emissivity

1. Introduction

Thermoforming is a method of manufacturing plastic parts by preheating a flat sheet of plastic to its forming temperature, then bringing it into contact with a mold whose shape it takes. The sheet is held against the mold surface unit until cooled. The formed part is then trimmed from the sheet.[1,2] Figure 1 shows the process of thermoforming.

Thermoforming is one of the most versatile and economical processes available for manufacturing returnable packaging and many other products. However, obtaining a uniform thickness of the final product with thermoforming is difficult. The adjustment of the heater power is very important because the thickness distribution is strongly dependent on the distribution of the sheet temperature. Table 1 shows the temperature of the forming window, which is the marginal temperature of the ABS sheet.[3] The uneven temperature of the upper and lower surfaces, and the thickness direction may cause defects such as cracks and wrinkles.

The focus of this paper is the control of the heating process. When the temperature of the ABS sheet exceeds the glass transition temperature in the heating process, the specific heat of the ABS sheet changes significantly, and the heat caused by radiation heat transfer and convection heat transfer also change. Nonlinear problems must

be considered because of the variation in the properties and operating conditions.[3] Initially, the steady-state optimum distribution of the heater power was determined by numerical optimization to obtain the uniform sheet temperature. If the final temperature of sheet is considered, then an unsteady-state analysis is required. To reduce the analysis time, the mean values of the initial and objective temperature were used in the calculation of the steady state. Using the response surface method, the time-dependent optimal variation of the heater input was determined to decrease the temperature difference between the surface and the center of the ABS sheet. The D-optimal method, one of the popular Design of Experiments (DOE) methods, was used to select experimental points.

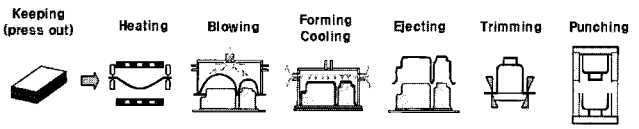

Fig. 1 Thermoforming process

Table 1 Forming window temperature

Forming Window	Lower Forming Temperature(°C)	Neutral Forming Temperature(°C)	Upper Forming Temperature(°C)
ABS Sheet	140	146	160
Objective	140	145	155

2. Analysis Model and Governing Equation

2.1 Analysis Model

In the preheating process, the ABS sheet is located as shown in Fig. 2. The size of sheet is 2 × 1 × 0.003 m. An array of 10 × 8 = 80 heaters exists on the upper and lower sides, and the heating time is 90 s. The distance between heaters and sheet is 0.2 m, and the temperature in the forming machine is set to 303 K. Convection between the heater and the outside is neglected. The power input to each heater during the heating time is q_{elec}.

The sheet and the heater are assumed to be diffuse gray surfaces, and the environment is considered to be a black body. The emissivities of the sheet and the heater are 0.85 and 0.9 respectively.

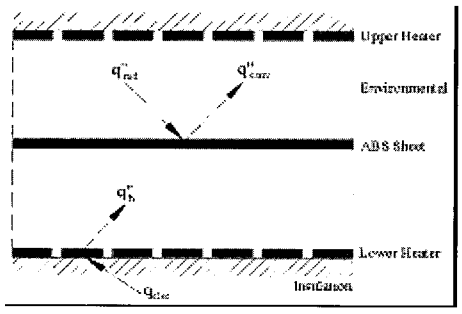

Fig. 2 Model schematic

2.2 Governing Equations

2.2.1 Radiation Heat Transfer

The net radiation method was used to calculate the radiation heat transfer. Equation (1) can be obtained using the heat from the heater and the surface temperature of the sheet,[4,5]

$$\sum_{j=1}^{N}\begin{cases}\delta_{kj}-F_{k-j}\\ \delta_{kj}-(1-\varepsilon_k)F_{k-j}\end{cases} J_j=\begin{cases}\dfrac{q_{h,k}}{A_k}-\sigma T_\infty^4 & 1\le k\le n_h\\ \varepsilon_k\sigma T_k^4-\sigma T_\infty^4 & n_h+1\le k\le N\end{cases} \quad (1)$$

where δ is the delta function, J_j is the radiosity of the jth element (W/m^2), $F_{k\,j}$ is the view factor from surface k to surface j, ε_k is the emissivity of the kth element, A_k is the area of k_{th} element (m^2), σ is the Stefan–Boltzmann constant (5.67 × 10^{-8} W m^{-2} K^{-1}), and T_∞ is the environmental temperature (K).

Using Eq. (2), the heat flux can be obtained using the calculated radiosity, and the heater temperature can be calculated using Eq. (3):

$$q''_{rad,j}=-\frac{\varepsilon_j}{1-\varepsilon_j}\left(\sigma T_j^4-J_j\right) \qquad j=n_h+1\sim N \quad (2)$$

$$T_j=\sqrt[4]{\left(\frac{\varepsilon_j}{1-\varepsilon_j}q''_j+J_j\right)\Big/\sigma} \qquad j=1\sim n_h \quad (3)$$

2.2.2 Convective Heat Transfer

Natural convection must be considered in analyzing the heating process in thermoforming.[6,7] The heat transfer coefficient (h) can be calculated using Goldstein, Lloyd, and Moran's correlation. Equations (4) and (5) can be used to calculate the heat transfer coefficient of the upper surface of the sheet, and Eq. (6) can be used to obtain the heat transfer coefficient of the lower surface of the sheet,[7] where k is the thermal conductivity (W m^{-1} K^{-1}):

$$\frac{\bar{h}L}{k}=0.54Ra_L^{1/4} \qquad \left(10^4\le Ra_L\le 10^7\right) \quad (4)$$

$$\frac{\bar{h}L}{k}=0.15Ra_L^{1/3} \qquad \left(10^7\le Ra_L\le 10^{11}\right) \quad (5)$$

$$\frac{\bar{h}L}{k}=0.27Ra_L^{1/4} \qquad \left(10^5\le Ra_L\le 10^{10}\right) \quad (6)$$

The characteristic length (L) is formulated as shown in Eq. (7), and the Rayleigh number (Ra_L) is as shown in Eq. (8):

$$L\equiv\frac{A_s}{P} \quad (7)$$

$$Ra_L=\left(\frac{g\beta(T-T_\infty)L^3}{\upsilon a}\right) \quad (8)$$

where P is the circumference (m), g is the acceleration of gravity (m/s^2), β is the volume expansion coefficient of air (K^{-1}), υ is the dynamic viscosity of air (m^2/s), and a is the thermal diffusivity of air (m^2/s).

The convective heat transfer from the sheet to the environment ($q'_{conv,j}$) is obtained by using the calculated heat transfer coefficient.

2.2.3 Conductive Heat Transfer

Conductive heat transfer is used to simulate the sheet heating process, which can be simplified to a one-dimensional problem through the direction of sheet thickness. Several different methods can be used in numerical simulation.[8-10] In this study, a fully implicit method is used as shown in Eq. (9), with the boundary condition in Eq. (10), where ρ is the density of the ABS sheet (kg/m^3):

$$\frac{T_i-T_i^{old}}{\Delta t}=\frac{k}{\rho C_p}\frac{T_{i+1}-2T_i+T_{i-1}}{\Delta z^2} \quad (9)$$

$$q''_{in,j}=q''_{rad,j}-q''_{conv,j} \qquad j=n_h+1\sim N \quad (10)$$

3. Optimal Heater Power Distribution of the Steady State

Not only the distribution of the heater power inputs in each position, but also the variations of the heater power inputs during the heating time, are important for obtaining a uniform temperature distribution of the ABS sheet. The optimal heater power distribution at steady state has been carried out at the first step. Using Eq. (11), the requirement of heat flux from the initial temperature (T_i) to the objective temperature (T_f) can be calculated.

$$q''_{req,j} = \frac{m_j}{2t_h A_j} \int_{T_i}^{T_f} C_p(T)dT \tag{11}$$

Figure 3 shows the temperature-dependent specific heat of the ABS sheet: where t_h is the heating time (s), m_j is the mass of the jth element (kg), and $C_P(T)$ is the temperature-dependent specific heat of the ABS sheet (J kg ^{1}K^{-1}).

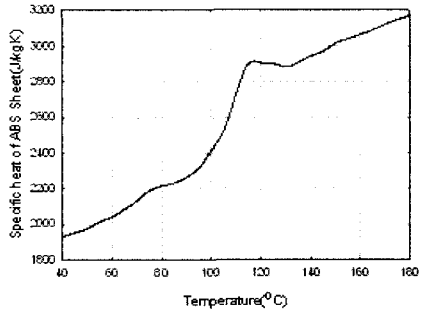

Fig. 3 Temperature-dependent specific heat of the ABS sheet

To determine the optimal distribution of heater power inputs for uniform temperature distribution, each heater power input is a design variable. The objective function was set as Eq. (12). The temperature of the sheet was set to $(T_i + T_f)/2$. In the steady state, only the calculation of the radiation heat transfer and the convective heat transfer is required. The constraints were set so that each heater input must be less than 80% of the maximum usable power (975 W). The optimization was carried out for both the upper and lower surfaces because the heat transfer coefficients of each surface are different. SQP was used as the optimization algorithm.[11,12]

$$f = \left[\sum_{j=n+1}^{N} \left(q''_{req,j} - q''_{in,j} \right)^2 \right]^{1/2} \Big/ N \tag{12}$$

The optimal results for each heater power input are shown in Tables 2 and 3, where the value for each position is the percent of 780 W (80% of maximum usable power).

Table 2 Heater power distribution of the upper surface for each position

100.0000	92.4810	98.3164	96.7570	96.7473	98.3185	92.4877	100.0000
72.0237	0	0	0	0	0	0	72.0251
0	8.8316	32.3100	25.3207	25.3541	32.3181	8.7968	0
81.9645	43.1142	32.1770	34.9269	34.8704	32.1337	43.2017	81.9565
32.9639	12.3788	25.1267	21.4794	21.5450	25.2010	12.2520	33.9837
33.9938	12.1742	25.4170	21.4219	21.3483	25.3423	12.2999	33.9657
81.9518	43.2477	31.9844	34.9563	35.0246	32.0251	43.1675	81.9680
0	8.7827	32.3773	25.3189	25.2815	32.3706	8.8113	0
72.0277	0	0	0	0	0	0	72.0232
100.0000	92.4869	98.3061	96.7532	96.7656	98.3028	92.4866	100.0000

Transient analysis was conducted to check the optimal result of the heater power distribution. Tables 4-6 show the temperature distribution of the upper surface, the lower surface, and the center of the ABS sheet, respectively. The heating time was 90 s. The mean values of the upper surface, the lower surface, and the center of the ABS sheet were 154.9°C, 157.2°C and 141.4°C, respectively, and the corner of the sheet center area had not reached the lower forming temperature (140°C). Additional optimization is required to reduce the temperature difference between the surface and the center.

Table 3 Heater power distribution of the lower surface for each position

100.0000	87.1805	94.3751	92.3631	92.3860	94.3616	87.1949	100.0000
64.3662	0	0	0	0	0	0	64.3734
0	10.5145	29.9864	24.1936	24.1023	30.0594	10.4359	0
80.8579	38.4693	31.5747	33.1536	33.3491	31.3937	38.6453	80.8356
31.0407	12.8849	23.5596	20.5639	20.3119	23.8230	12.6683	31.0772
31.0774	12.6585	23.8362	20.3227	20.5692	23.5560	12.8437	31.0458
80.8435	38.6280	31.3748	33.3351	33.1514	31.5977	38.5116	80.8535
0	10.4511	30.0710	24.1114	24.1936	29.9655	10.4965	0
64.3716	0	0	0	0	0	0	64.3686
100.0000	87.1922	94.3571	92.3847	92.3652	94.3809	87.1835	100.0000

Table 4 Temperature distribution of the upper surface

150.6	154.1	153.8	151.0	154.0	153.8	154.1	150.6
157.4	156.4	156.1	156.2	156.2	156.1	156.1	157.4
153.0	153.6	154.5	154.5	154.5	154.5	153.6	153.0
155.3	156.2	156.1	156.2	156.2	156.1	156.2	155.3
154.6	155.2	155.5	155.6	156.6	155.5	155.2	154.6
154.6	155.2	155.5	155.6	155.6	155.5	155.2	154.6
155.3	156.2	156.1	156.2	156.2	156.1	156.2	155.3
153.0	153.6	154.5	154.5	154.5	154.5	153.6	153.0
157.4	156.4	156.1	156.2	156.2	156.1	156.4	157.4
150.6	154.1	153.8	154.0	154.0	153.8	154.1	150.6

Table 5 Temperature distribution of the lower surface

152.9	156.3	156.0	156.2	156.2	156.0	156.3	153.9
159.5	158.7	158.4	158.5	158.5	158.4	158.9	159.5
155.1	155.9	156.7	156.7	156.7	156.7	156.0	156.2
157.6	158.5	158.4	158.5	158.5	158.4	158.5	157.6
156.7	157.4	157.8	157.9	157.9	157.8	157.4	156.7
156.7	157.4	157.8	157.9	157.9	157.9	157.4	156.5
157.6	158.5	158.4	158.5	158.5	158.4	158.5	157.6
155.1	155.9	156.7	156.7	156.7	156.7	155.9	155.1
159.5	158.7	158.4	158.5	158.5	158.4	158.9	159.5
152.9	156.2	156.0	156.2	156.2	156.0	156.3	152.9

Table 6 Temperature distribution of the center

138.2	140.9	140.6	140.7	140.7	140.6	140.9	138.2
143.7	142.7	142.4	142.4	142.4	142.4	142.7	143.7
139.9	140.2	140.8	140.8	140.8	140.8	140.2	139.9
141.8	142.3	142.1	142.2	142.2	142.1	142.3	141.8
141.1	141.4	141.6	141.6	141.6	141.6	141.4	141.1
141.1	141.4	141.6	141.6	141.6	141.6	141.4	141.1
141.9	142.3	142.1	142.2	142.2	142.1	142.3	141.8
139.9	140.2	140.8	140.8	140.8	140.8	140.2	139.9
143.7	142.4	142.4	142.4	142.4	142.4	142.7	143.7
138.2	140.9	140.6	140.7	140.7	140.6	140.9	138.2

4. Optimal Time-Dependent Variation in Heater Power Input

Optimization must be connected with transient thermal analysis to determine the optimal variation in the heater power inputs. If the analysis code were directly connected to the optimization code, the optimization time would be very long. In this study, the response surface method was used to reduce the optimization time.

4.1 Response Surface Method Concept

The response surface methodology is a widely used tool in the quality engineering field.[13,14] The response surface methodology comprises regression surface fitting to obtain approximate responses, DOE to obtain minimum variances of the responses, and optimizations using the approximated responses.[15] For most of the response surfaces, the functions for the approximations are polynomials because of their simplicity, although the functions are not limited to the polynomials. In this study, the response surface was composed of the quadratic polynomials in Eq. (13) to set up a smooth curved surface:

$$C_m(x_i) = c_0 + \sum_{i=1}^{k} c_i x_i + \sum_{i=1}^{k} c_{ii} x_i^2 + \sum_{i=1}^{k-1} \sum_{j=2}^{k} c_{ij} x_i x_j \qquad (13)$$

where $C_m(x)$ is the objective function, c_i is the coefficient to be defined, and K is the number of design variables. When the response model is defined as a quadratic polynomial, the number of coefficients c_i can be expressed as $(k + 1)(k + 2)/2$.

The adjusted coefficient of the multiple determination (R^2_{adj}) is used to judge the goodness of the approximation of the response surface. The R^2_{adj} has a maximum value of 1 and a minimum value 0. The value is closer to 1 for a better response surface.

For problems that have complicated constraints or when the design space is not rectangular, the conventional DOE methods such as the orthotropic designs cannot be applied, and computer-aided DOE methods are the only candidates. D-optimal design is one of these popular computer-aided DOE methods. In this study, the D-optimal method was used in the process of selecting experimental points for setting up the response surface.

4.2 Construction of the Response Surface

In this study, the total heating time (90 s) was divided into three steps, and the design variables were the ratios of the calculated steady-state heater power inputs of the three steps. Table 7 shows the lower and upper boundaries of the design variables. The mean temperature of the lower surface, the mean temperature of the center, and the mean difference of the temperature through the thickness direction were selected for constructing response surfaces. For improving the reliability of the response surface method, 15 experimental points were selected using the D-optimal DOE method as shown in Table 8; this is 1.5 times the number of the unknown coefficients. The calculated unknown coefficients are listed in Table 9. As an evaluation standard for the reliability of the response, the value of R^2_{adj} in each constructed response surface is greater than 0.98, or very close to 1.

Table 7 Lower and upper bounds for each design variable

Design variables	Minimum value	Maximum value
Ratio for step 1 (0–30 s)	0.8	1.2
Ratio for step 2 (30–60 s)	0.8	1.2
Ratio for step 3 (60–90 s)	0.8	1.2

Table 8 Analysis results of the selected experimental points

No	Step 1	Step 2	Step 3	Temp difference (°C)	Mean temp of the lower surface (°C)	Mean temp of the center (°C)
1	0	0	0	15.8	157.2	141.4
2	0	1	0	15.6	162.1	146.5
3	1	0	–1	12.1	153.8	141.7
4	1	0	0	15.6	161.7	146.1
5	1	0	1	19.2	169.5	150.3
6	–1	0	0	16.0	152.6	136.6
7	0	–1	0	16.0	152.2	136.2
8	1	–1	0	15.9	156.8	140.9
9	1	1	1	18.9	174.3	155.4
10	–1	1	–1	12.2	149.6	137.4
11	0	–1	1	19.5	160.1	140.6
12	–1	–1	–1	12.7	139.5	126.8
13	0	–1	–1	12.5	144.2	131.7
14	1	1	–1	11.8	158.7	146.9
15	–1	–1	1	19.8	155.6	135.8

Table 9 Coefficients for the constructed response surface

No	Coefficient for the maximum difference of the temperature	Coefficient for the mean temperature of the lower surface	Coefficient for the mean temperature of the center
1	0.157874E+02	0.157178E+03	0.141391E+03
2	–0.203118E+00	0.453791E+01	0.474102E+01
3	–0.228701E+00	0.494391E+01	0.517261E+01
4	0.355673E+01	0.792155E+01	0.436482E+01
5	0.399952E-01	–0.164793E-01	–0.564745E-01
6	–0.913909E-03	–0.255702E-01	–0.246563E-01
7	0.457597E-02	–0.501767E-01	–0.547527E-01
8	–0.326502E-01	–0.636042E-01	–0.309541E-01
9	–0.312191E-01	–0.792580E-01	–0.480389E-01
10	0.412191E-01	–0.407420E-01	–0.819611E-01

4.3 Optimal Results Using the Response Surface Method

The optimal design was achieved to decrease the mean temperature difference through the direction of thickness using the constructed response surface. The constraint was that the mean temperature of each position through the direction of thickness must be in the forming temperature range. In this study, the lower forming temperature was set as 140°C, and upper forming temperature was set as 155°C.

Table 10 Comparison of optimal heating and uniform heating by checking the accuracy of the optimal results using the response surface method

Item	Step 1 (0–30 s)	Step 2 (30–60 s)	Step 3 (60–90 s)	Temp difference (°C)	Mean temp of the lower surface (°C)	Mean temp of the center (°C)
Uniform heating	1.0	1.0	1.0	15.8	157.2	141.4
Optimal Heating	1.0365944	1.2	0.8	11.9	155.0	143.1
Analysis results	1.0365944	1.2	0.8	12.0	155.0	143.0

Figures 4(a)-(c) show the distribution of temperature in the lower and upper surfaces, and the distribution of the mean temperature of the final optimal results. Figure 5 shows that a difference in temperature exists between the surface and the center of the ABS sheet, but this difference is much smaller than in the case of uniform preheating. The accuracy of the optimal results using the constructed response surface was verified as shown in Table 10. Unnecessary iterative analysis time can be reduced by using the response surface method and optimization techniques.

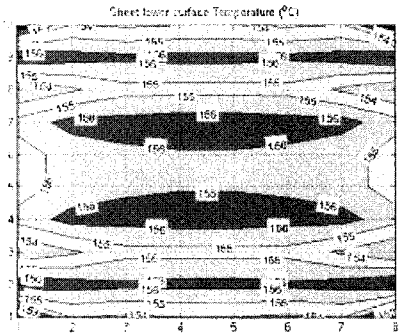

Fig. 4 (a) Temperature distribution of the lower surface

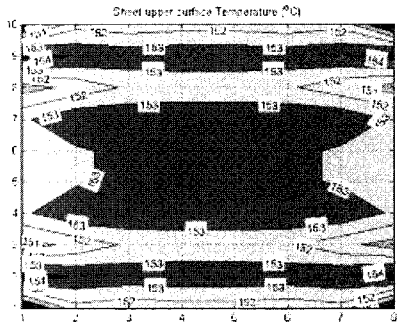

Fig. 4 (b) Temperature distribution of the upper surface

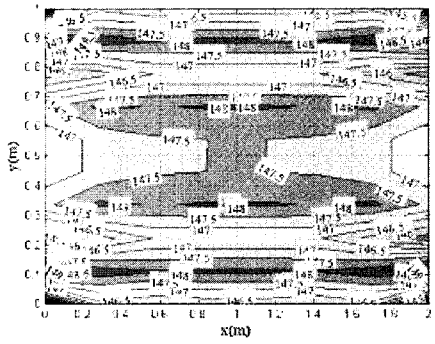

Fig. 4 (c) Temperature distribution of the mean temperature

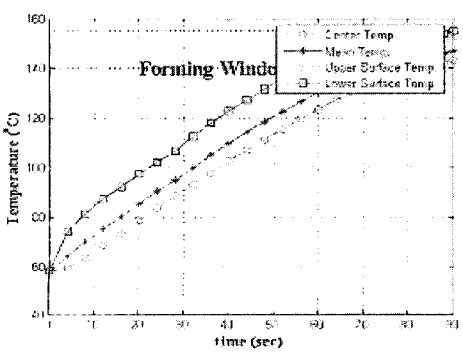

Fig. 5 Time-dependent variation in temperature

5. Conclusions

The analysis code for simulating the heating process was developed. To obtain a uniform temperature distribution, the optimal distribution of heater power inputs was first determined by setting the temperature of the sheet to the mean value of the initial and objective temperatures. To decrease the temperature difference between the surface and the center of the sheet, the optimal time-dependent heater power inputs were determined using the constructed response surface. The D-optimal method was used to select experimental points. The optimal results show that the time-dependent optimum heater power distribution produces an acceptable uniform sheet temperature in the forming temperature range by the end of the heating process.

REFERENCES

1. Warby, M. K., Whiteman, J. R., Jiang, W. G., Warwick, P. and Wright, T., "Finite element simulation of thermoforming processes for polymer sheets," Mathematics and Computers in Simulation, Vol. 61, No. 3-6, pp. 209-218, 2003.

2. Cunningham, J. E., Monaghan, P. F. and Brogan, M. T., "Predictions of the temperature profile within composite sheets during pre-heating," Applied Science and Manufacturing, Vol. 29, No. 1-2, pp. 51-61, 1998.

3. Throne, J. L., "Technology of thermoforming," Hanser Publishers, Munich, pp. 1-53, 1987.

4. Brogan, M. T. and Monaghan, P. F., "Thermal simulation of quartz tube infrared heater used in the processing of thermoplastic composites," Applied Science and Manufacturing, Vol. 27, No. 4, pp. 301-306, 1995.

5. Zhang, Z. M. and Zhou, Y. H., "An effective emissivity model for rapid thermal processing using the net radiation method," International Journal of Thermophysics, Vol. 22, No. 5, pp. 1563-1575, 2001.

6. Goldstein, R. J., Sparrow, E. M. and Jones, D. C., "Natural convection mass transfer adjacent to horizontal plates," Int. J. Heat and Mass Transfer, Vol. 16, pp. 1025-1037, 1973.

7. Lloyd, J. R. and Moran, W. R., "Natural Convection Adjacent to Horizontal Surfaces of Various Plan Forms," Journal of Heat Transfer, Vol. 96, pp. 443-451, 1974.

8. Lee, Y. S., Kang, T. J. and Lee, J. K., "A study on heat transfer through plain woven fabric. An approach through finite difference method," Journal of the Korean Fiber Society, Vol. 28, No. 9, pp. 707-714, 1991.

9. Oh, J. E., Lee, C. H., Sim, H. J., Lee, H. J., Kim, S. H. and Lee, J. Y., "Development of a system for diagnosing faults in rotating machinery using vibration signals," International Journal of Precision Engineering and Manufacturing, Vol. 8, No. 3, pp. 54-59, 2007.

10. Sahin, M. and Wilson, H. J., "A semi-staggered dilation-free finite volume method for the numerical solution of viscoelastic fluid flows on all-hexahedral elements," Journal of Non-Newtonian Fluid Mechanics, Vol. 147, No. 1-2, pp. 79-91, 2007.

11. Li, Z. Z., Shen, Y. D., Heo, K. S., Lee, J. W., Seol, S. Y., Byun, Y. H. and Lee, C. J., "Feasible optimal design of high temperature vacuum furnace using experiences and thermal analysis database," Journal of Thermal Science and Technology, Vol. 2, No. 1, pp. 123-133, 2007.

12. Li, Z. Z., Park, M. Y., Lee, J. W., Byun, Y. H. and Lee, C. J., "Optimal design of high temperature vacuum furnace using thermal analysis database," Transaction of the KSME B, Vol. 30, No. 6, pp. 594-601, 2006.

13. Youn, B. D., "An integrated design process for manufacturing and multidisciplinary design under system uncertainty," International Journal of Precision Engineering and Manufacturing, Vol. 5, No. 4, pp. 61-68, 2004.

14. Lee, T. W. and Reitz, R. D., "Response surface method optimization of a HSDI diesel engine equipped with a common rail injection system," ASME, Vol. 37-1, pp. 89-95, 2001.

15. Chun, D. M., Kim, M. H., Lee, J. C. and Ahn, S. H., "A nano-particle deposition system for ceramic and metal coating at room temperature and low vacuum conditions," International Journal of Precision Engineering and Manufacturing, Vol. 9, No. 1, pp.51-53, 2008.